Title

Selective activation of serotoninergic dorsal raphe neurons facilitates sleep through anxiolysis.

Permalink

https://escholarship.org/uc/item/5hh6w7rb

Journal

Sleep, 43(2)

ISSN

0161-8105

Authors

Venner, Anne
Broadhurst, Rebecca Y
Sohn, Lauren T
et al.

Publication Date

2020-02-01

DOI

10.1093/sleep/zsz231

Peer reviewed

ORIGINAL ARTICLE

Selective activation of serotoninergic dorsal raphe neurons facilitates sleep through anxiolysis

Anne Venner[1,2,†], Rebecca Y. Broadhurst[1,2,†], Lauren T. Sohn[1,2], William D. Todd[3,4] and Patrick M. Fuller[1,2,*]

[1]Department of Neurology, Beth Israel Deaconess Medical Center, Boston, MA, [2]Division of Sleep Medicine, Harvard Medical School, Boston, MA, [3]Department of Zoology and Physiology, University of Wyoming, Laramie, WY and [4]Program in Neuroscience, University of Wyoming, Laramie, WY

[†]These authors contributed equally to this work.

*Corresponding author. Patrick M. Fuller, Department of Neurology, Beth Israel Deaconess Medical Center, E/CLS 707, 3 Blackfan Circle, Boston, MA 02115. Email: pfuller@bidmc.harvard.edu.

Abstract

A role for the brain's serotoninergic (5HT) system in the regulation of sleep and wakefulness has been long suggested. Yet, previous studies employing pharmacological, lesion and genetically driven approaches have produced inconsistent findings, leaving 5HT's role in sleep-wake regulation incompletely understood. Here we sought to define the specific contribution of 5HT neurons within the dorsal raphe nucleus (DRN[5HT]) to sleep and arousal control. To do this, we employed a chemogenetic strategy to selectively and acutely activate DRN[5HT] neurons and monitored sleep-wake using electroencephalogram recordings. We additionally assessed indices of anxiety using the open field and elevated plus maze behavioral tests and employed telemetric-based recordings to test effects of acute DRN[5HT] activation on body temperature and locomotor activity. Our findings indicate that the DRN[5HT] cell population may not modulate sleep-wake per se, but rather that its activation has apparent anxiolytic properties, suggesting the more nuanced view that DRN[5HT] neurons are sleep permissive under circumstances that produce anxiety or stress.

Statement of Significance

Although decades of research have suggested a critical role for the brain's serotoninergic system in regulating behavioral state, the precise contribution of the dorsal raphe serotonin (DRN[5HT]) neurons to sleep and arousal control has remained incompletely understood. We show here, for the first time, that in vivo activation of DRN[5HT] neurons in mice produces a modest increase in sleep. We furthermore show that this evoked increase in sleep is likely secondary to an anxiolytic effect of activating the DRN[5HT] cell population. Future research directed at uncovering the neural circuitry through which dorsal raphe serotonin neurons produce anxiolysis to facilitate sleep may inform the development of newer therapeutic interventions for patients with anxiety, in particular, those patients experiencing comorbid insomnia.

Key words: chemogenetics; mice; EEG/EMG; serotonin; dorsal raphe; AAV; anxiety; stress; thermoregulation

Introduction

Serotonin (5HT)-containing neurons of the brain's raphe nuclei are linked to the regulation of many neurobiological and physiological processes, including sleep-wake behaviors [1]. For example, early electrolytic lesion and pharmacological studies in cats determined that 5HT promotes sleep, a finding that informed the seminal monoaminergic theory of sleep and waking [2]. However, subsequent electrophysiological and microdialysis studies, which focused on the dorsal raphe nucleus (DRN), found that DRN neurons, including putative 5HT DRN (DRN5HT) neurons, fire predominantly during wake, decrease their firing activity during non-REM (NREM) sleep and become virtually silent during REM sleep. This pattern of DRN cell activity was also found to correlate positively with state-dependent 5HT levels within the brain [3–8]. Collectively these data informed a revised model in which DRN5HT neurons promote wakefulness. Subsequent studies provided an anatomic framework for this newer model, showing, for example, that DRN5HT neurons are reciprocally connected with multiple brain regions involved in arousal state control [9–14], including the sleep-promoting ventrolateral preoptic nucleus, where 5HT was initially found to be mostly inhibitory [15]. DRN5HT neurons have since assumed their place as an important wake-promoting component of the highly influential sleep-wake "flip-flop" switch model [16].

Sleep-wake studies in 5HT receptor knock-out models have also indicated a role for 5HT in sleep-wake regulation. For example, global developmental knock-out of the inhibitory $5HT_{1A}$ and $5HT_{1B}$ receptors increases REM sleep [17, 18], whereas selective knockout of the $5HT_{1A}$ receptor in wake-stabilizing orexin neurons of the lateral hypothalamus increases NREM sleep [19]. Conversely, knock-out of other 5HT receptors has been shown to produce no effect or opposite effects upon sleep-wake [20].

Altogether, available evidence continues to support a role for central 5HT in modulating sleep and arousal, although the specific role that DRN5HT neurons play in these processes remains incompletely understood. A more detailed understanding of how central 5HT, and specifically DRN5HT, regulates sleep and arousal has also been hampered by the fact that manipulations of the 5HT system influence other neurobiological processes, which themselves may impact sleep and wake. For example, dysfunction of the central 5HT system is likely a major contributing etiology to many mood disorders, including anxiety and depression, and sleep disturbances are a common comorbidity in these disorders [21–23]. In contrast, chronic sleep disruption can precipitate mood disorders [24], suggesting a strong and bidirectional interrelationship between sleep and mood disorders.

Here, and with the goal of defining the specific contribution of DRN5HT neurons to sleep-wake control, we employed a chemogenetic strategy to selectively and acutely activate 5HT neurons in the DRN, and monitored sleep-wake using electroencephalogram recordings. To provide additional context for our data interpretation, we also measured indices of anxiety using the open field and elevated plus maze behavioral tests, following chemogenetic activation of DRN5HT neurons, and carried out telemetric-based recordings to determine if acute activation of DRN5HT neurons altered locomotor activity or body temperature, both of which vary as a function of behavioral state.

Methods

Animals

Adult male (8–12 weeks) transgenic SERT-Cre mice were used in this study. SERT-Cre mice (RRID: MMRRC_017260-UCD) were generated with a modified bacterial artificial chromosome (BAC)-Cre construct encoding the serotonin transporter gene (Slc6a4, SERT) [25]. All mice were bred and housed in our animal facility, genotyped before and after experiments, maintained in a 12-hour light/dark cycle, and had ad libitum access to food and water. All procedures were approved by the Institutional Animal Care and Use Committee of Beth Israel Deaconess Medical Center.

Mouse validation

To validate the selectivity of the SERT-Cre mouse, we crossed SERT-Cre to lox-STOP-lox-GFP-L10 reporter mice [26] and immunolabeled Cre-driven L10-GFP and 5HT to assay for specificity and penetrance of Cre-recombinase expression. Mice were sacrificed and tissues processed for L10-GFP and 5HT, as detailed below. Clearly labeled L10-GFP (green), 5HT (magenta), and double-labeled L10-GFP and 5HT (white) positive nuclei were counted within 5HT cell populations using a cell count plugin in Fiji (Fiji Is Just ImageJ) [27] to mark counted cells. Where possible, 5HT cell populations were classified as previously described by Hornung [28], with some specified exceptions. The B9 cell population, originally described as a single entity by Dahlstrom and Fuxe [29], was later characterized by Vertes and Crane [30] as comprising a supraleminiscal (SuL) group and a more dispersed group within the pontomesencephalic nucleus of the rat (analogous to the pontine reticular nucleus, oral part (PnO), of the mouse, as described in the mouse atlas of Franklin and Paxinos [31]). We have adopted the Vertes and Crane definitions of the B9 area for our mouse line validation study. Additionally, 5HT neurons observed in the interpeduncular nucleus (IP; medial to the supralemisical group) were considered as part of the rostral pole of the median raphe (MnR) whereas neurons in the pontine raphe were considered as part of the caudal MnR. Finally, 5HT neurons in the lateral paragigantocellular reticular nucleus (LPGi), though arguably a caudo-lateral extension of the raphe magnus (RMg), are treated as a discrete subpopulation for the purpose of our mouse line validation study.

Surgery

Prior to surgery, mice were anesthetized with ketamine/xylazine (100 mg/kg and 10 mg/kg, respectively, i.p.) and received 4 mg/kg meloxicam SR subcutaneously for pain relief. The top of the mouse's head was shaved before it was placed into a stereotaxic frame. Next, the skin over the skull was sterilized with betadine and 70% isopropyl ethanol before an incision was made down the midline of the skull. The skin was retracted, exposing lambda and bregma so that the head could be leveled. A burr hole (0.7 mm diameter) was drilled immediately above the DRN and an incision made in the meningeal layer with a 25G needle. To selectively express hM3Dq in DRN5HT neurons, we injected 30–60 nl of an adeno-associated viral (AAV) vector expressing the hM3Dq-mCherry receptor (hSyn-DIO- hM3Dq-mCherry- AAV10) into the DRN (AP = –4.4 mm; ML = 0.0 mm; DV

= −2.25 mm) using a compressed air delivery system (adapted from Amarel and Price [32]). Briefly, a small diameter micropipette (0.275 mm internal diameter, P-.275M-1M-1–12, Wilmad LabGlass) was pulled using a Narashige PE-2 micropipette puller and the opening was trimmed with a pair of sharp forceps so that they gradually tapered a to 10–20 μm opening. The micropipette was filled with the viral vector and connected to the output port of a solenoid (Clippard, CR-EV-3-24-L) with 1/16″ internal diameter PVC tubing. Positive pressure was applied to the input port of the solenoid, using a regulated air supply from a compressed air tank (Linde Medical Gas UN 1002, with Western Digital M1-346-PG regulator), such that the pressure for each puff was ~30 psi. A Grass S44 stimulator was connected to the solenoid using a UHF male-BNC female adaptor and BNC screwhead splitter and triggered the solenoid to dispel the viral vector at a rate of 0.8–1 Hz (equating to ~ 0.5 nl per second). Following the intracranial injection, we waited for 3 minutes to allow the viral vector to disperse before gently withdrawing the micropipette from the brain. The scalp incision was closed with Vetbond, 0.5 ml saline was administered subcutaneously and the mouse was allowed to regain consciousness on a heating pad.

Mice recovered for 2 weeks post-brain injection and then underwent a second surgery to implant a headstage for recording the electroencephalogram (EEG) and electromyogram (EMG). The headstage consisted of a six-pin connector (Heilind Electronics, Inc. catalog #MMX853-43-006-10-001000) soldered to four EEG screws (Pinnacle, catalog #8403) and two flexible EMG wire electrodes (Plastics One, catalog #E363). Mice were prepared for surgery as described above and four burr holes (0.7 mm diameter) were drilled in the skull: two anterior burr holes were drilled at AP: +1.0 mm and ML: ± 1.0 mm and two posterior burr holes were drilled at AP: −2.0 and ML: ± 1.0. The EEG electrode screws were inserted into the burr holes and affixed to the skull with a layer of dental cement mixed with cyanoacrylate glue. The EMG electrodes were guided down the back of the neck underneath the trapezius muscle. The whole assembly was coated in a layer of dental cement to provide insulation and structural stability. The mice recovered for an additional 2 weeks following implantation of the EEG/EMG connector. For mice used in body temperature and locomotor activity recordings (n = 5), an incision was made in the i.p. cavity and a biotelemetry transmitter (TA-F10, Data Sciences International) was implanted. Incisions were sutured and treated by topical antibiotic.

Sleep-wake monitoring

Four weeks after injection of the viral vector, the mice (n = 18) were housed individually in transparent barrels in an insulated sound-proofed recording chamber, maintained at an ambient temperature of 22 ± 1°C and on a 12-hour light/dark cycle (lights on at 6:00 am, Zeitgeber time: ZT0), with food and water available ad libitum. Mice were habituated to the recording cable for 4 days before starting polysomnographic recording. During this habituation period, mice were picked up and handled once a day. Mice were recorded for a 24-hour baseline period and then injected with the hM3Dq ligand, Clozapine-N-Oxide (CNO; 0.3 mg/kg in saline, i.p., NIMH) at 9:00 am (ZT3, light period, time of high sleeping drive) or at 6:00 pm (ZT12, lights-off, time of high waking drive). After each CNO injection, there was a 48-hour washout period. As an injection control, mice were also injected with saline at 9:00 am and 6:00 pm using a within-subject design.

Sleep recording and analysis

Cortical EEG (ipsilateral frontoparietal) and EMG signals were amplified by x5000, filtered (0.3 Hz: 20 kHz) and digitized at a resolution of 500 Hz using Vital Recorder (Kissei Comtec). Polysomnographic records were visually scored using SleepSign for Animal 2 (Kissei Comtec) in 10-second epochs for wakefulness (W), rapid eye movement (REM), and non-REM (NREM) sleep and the percentage of time spent in W, REM, and NREM sleep was calculated for each mouse. The latency to NREM following CNO or saline injection was calculated by subtracting the time of the injection from the time of the first NREM episode lasting 10 seconds or longer. Fragmentation analyses and baseline comparison of the percentage of time spent in W, REM, and NREM sleep were carried out for the first 2 hours following CNO or saline injection at ZT3 and ZT12.

To perform an EEG power spectrum analysis, recordings were re-scored in 5-second epochs for a 1.5-hour period (0.5–2 hours post saline and CNO injection) and processed using a Fast Fourier Transform (FFT) routine as described previously [33]. Briefly, epochs containing artifacts occurring during active wake (with large movements) or containing two vigilance states were visually identified and omitted from the spectral analysis, and recordings that had wake artifact more than 20% of the time were removed from the spectral analysis. The data were normalized by expressing each frequency bin as a percentage relative to the same bin in baseline condition from the same mouse and from the same time of day. To analyze the EEG frequency bands, relative power bins were summed in δ = 0.5–4 Hz, low θ = 4–6 Hz, high θ = 6–10 Hz, α = 10–20 Hz, γ = 20–50 Hz, high γ = 70–200 Hz.

Behavioral testing

All behavioral tests were administered between 9:00 am and 1:00 pm. Mice (n = 20) were brought into the test room and habituated for at least 60 minutes before the start of the experiment. The illumination level in the test room was maintained at 135 lux. All mice were first tested in the open field and then the elevated plus maze. Mice were tested in a randomized crossover design. Behavioral testing began 10 minutes after injection of either CNO (0.3 mg.kg in saline [i.p.] or saline [i.p.]).

Open field test

For this test, mice were placed into the center of a large square chamber (48.5 × 48.5 × 30 cm) made of grey KOMATEX and were allowed to freely explore the chamber for 10 minutes while their movement was tracked and recorded by EthoVision 8.5 tracking software (Noldus). The center was defined as a square comprised of 50% of the total area of the chamber. Time spent in the surround vs. the center was the primary measure of anxiety behavior as mice typically spend a significantly greater amount of time exploring the periphery rather than the unprotected center area. Once the test was completed, mice were returned to their

home cage. The chamber was cleaned with Clidox (Pharmacal Research Laboratories) between each trial.

Elevated plus maze

For this test, mice were placed at the center of the elevated plus maze. The maze apparatus was made from white Plexiglas and consists of two opposing open arms (60.5 × 7 cm) and two opposing closed arms (60.5 × 7 × 12 cm), arranged in a plus configuration and elevated 75 cm. During the 10 minutes of free exploration, their movements were tracked by EthoVision 8.5 software tracking (Noldus). The primary measure of anxiety behaviors was the time spent in the closed arms vs. the open arms as mice tend to avoid the open areas and favor darker and more enclosed areas. After the trial, mice were returned to their home cage. The maze was cleaned with Clidox between each trial.

Telemetry recordings

Body temperature and locomotor activity telemetry recordings ($n = 5$) followed all behavioral tests. Mice were individually housed in standard plastic cages inside isolation chambers with ad libitum food and water. Cages were placed atop telemetry receivers interfaced to a microcomputer data acquisition system (Data Sciences International). Mice were habituated to these chambers for at least 3 days before recording. Body temperature values were recorded at 5-minute intervals, and locomotor activity data were collected in 5-minute bins.

Immunohistochemistry

Animals were injected with either CNO (0.3 mg/kg in saline, i.p.) or saline (i.p.) at 9:00 am. Ninety minutes later mice were deeply anesthetized with 200 mg/kg chloral hydrate and transcardially perfused with 20 mL saline followed by 100 mL of neutral phosphate buffered formalin (4%, Fisher Scientific). Brains were removed and incubated in 20% sucrose at 4°C until they sank, then sectioned at 40 µm on a freezing microtome in three series. Brain sections were washed in phosphate buffered saline (PBS), and incubated in primary antiserum (dsRed rabbit polyclonal antibody [1:10K; Clontech; catalog number 632496]), and/or c-Fos rabbit polyclonal antibody (1:15K; Oncogene Sciences, catalog number 4188), or 5-HT goat polyclonal antibody (1:5K; Immunostar, catalog number 20079) diluted in PBS containing 0.3% Triton X-100 (PBST) and 0.2% sodium azide overnight at room temperature. To detect primary antibodies, sections were washed in PBS and incubated in biotinylated secondary antiserum (against appropriate species IgG, 1:1000, Jackson ImmunoResearch) in PBST for 2 hours, washed in PBS and incubated in ABC reagents (1:1000, Vectastain, Vector Laboratories) in PBST for 1 hour. Sections were washed again and then reacted in a solution of 0.02% 3,3-diaminobenzidine tetrahydrochloride (DAB, Sigma) and 0.009% hydrogen peroxide. The sections were stained brown with DAB or black (to visualize c-Fos) by DAB plus 0.005% cobalt chloride and 0.01% nickel ammonium sulfate. For fluorescent detection of primary antibodies, sections were washed 3 times in PBS and incubated in fluorescent secondary antiserum for 2 hours (against appropriate species IgG, 1:500, Jackson ImmunoResearch).

All sections were then washed twice in PBS-Azide and then mounted on positively charged slides (Denville Scientific, Inc.). Histology was imaged using an Olympus BX61VS slide scanner. To construct heatmaps of the injection sites, brain sections were aligned using the DRN as a reference and the injection site for each mouse projected onto a series of standardized sections. Heatmaps (consisting of overlaid injection sites for each mouse) were then generated using a custom-written Python script [34].

In images using both red and green fluorophores, the red channel was false-colored to magenta using Fiji for the benefit of the color-blind population.

Statistical analysis

All data are presented as the mean ± standard error of mean (SEM). Sample size and power calculations were performed post hoc using PS Power and Sample Size Calculations by William D. Dupont and Walton D. Plummer (http://biostat.mc.vanderbilt.edu/PowerSampleSize) using means and standard deviations derived from our analysis. Statistical analysis was performed using Prism v6 (GraphPad Software). Differences with $p < 0.05$ were considered significant. Data were tested for normality using the D'Agostino-Pearson test prior to carrying out statistical analyses. When examining the effect of CNO injections upon sleep-wake over time and upon the EEG spectra, two-way ANOVA for repeated measures followed by Sidak post hoc tests were carried out. Percentage of NREM, wake, and REM between baseline conditions (same time of day without an i.p. injection), saline injection, and CNO injection were compared by one-way ANOVA. Latency to sleep, sleep fragmentation analyses and open field and elevated plus maze analyses were all compared with two-tailed paired t-tests or (for data that was nonparametric), Wilcoxon matched-pairs signed rank test.

Results

Conditional activation of DRN^5HT neurons reduces the latency to NREM sleep

To investigate the role of DRN^5HT neurons in regulating arousal, we utilized the SERT-Cre mouse generated by the GENSAT project [25]. We first validated the selectivity of this mouse line by crossing SERT-Cre to lox-STOP-lox-GFP-L10 reporter mice [26] and immunolabeling Cre-driven L10-GFP and 5HT to assay for specificity and penetrance of Cre expression (Figure 1). We confirmed that L10-GFP expression exhibited a high degree of colocalization with 5HT in all anatomically defined serotoninergic subpopulations (Figure 1A–G), indicating that the Cre expression was both highly penetrant and specific to 5HT neurons. Within the DRN, we counted n = 1138 L10-GFP neurons in the dorsal DRN (95.5% of the local population of 5HT neurons), $n = 999$ L10-GFP neurons in the ventral DRN (97.1% of the local 5HT population) and $n = 1352$ L10-GFP neurons in the lateral wings of the DRN (90.2% of the local 5HT population), indicating that the distribution of Cre-expressing neurons within DRN subunits was fairly uniform. We observed little ectopic expression of L10-GFP in non-serotoninergic nuclei although occasional isolated neurons (<12 in any one brain region) were scattered throughout the brain. Additionally,
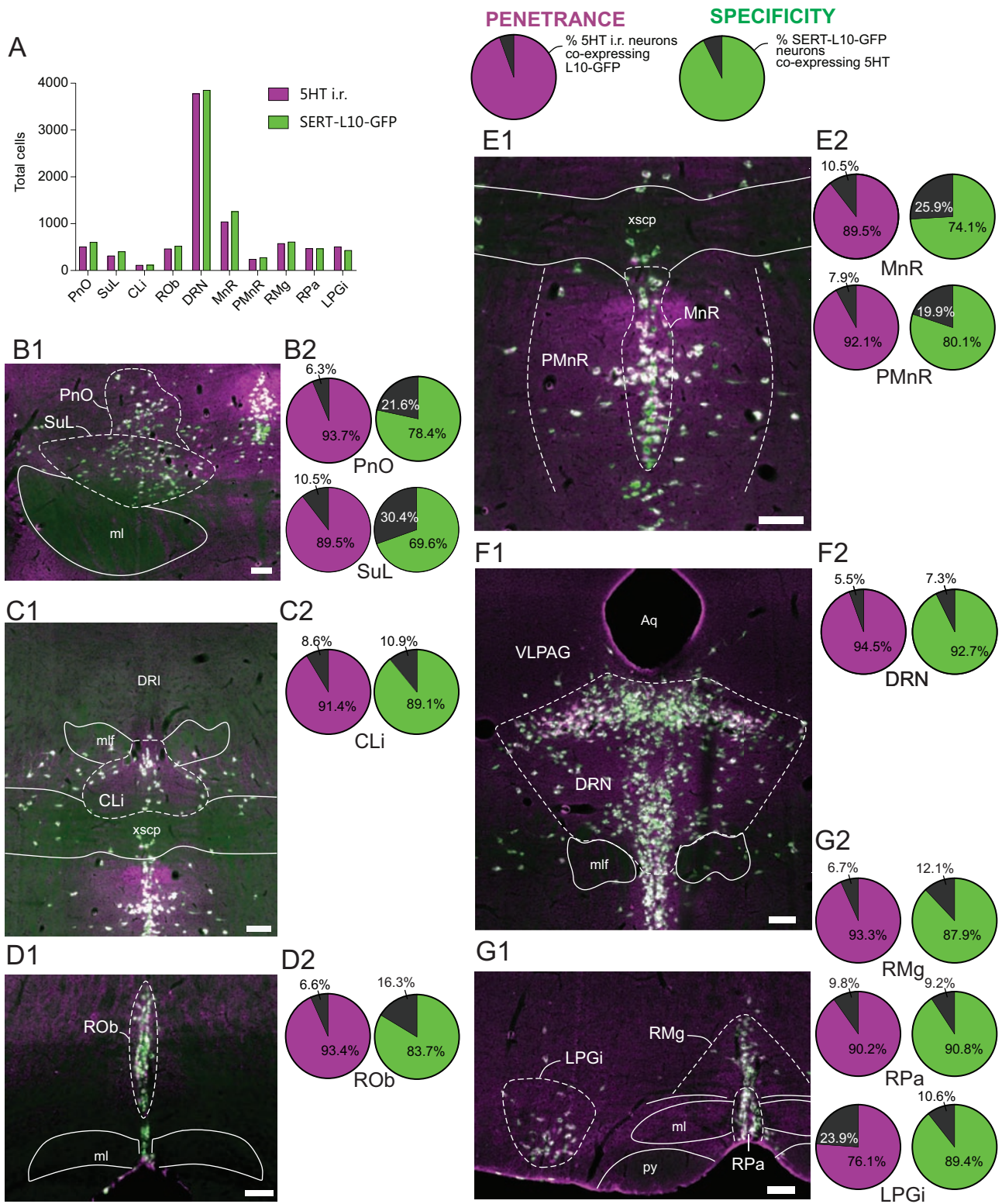
Figure 1. Validation of the SERT-cre mouse line. (A) Total number of 5HT immunoreactive (i.r.) neurons and SERT-L10-GFP neurons counted per brain region. (B–G) Left: Photomicrographs illustrating 5HT i.r. (magenta) and SERT-L10-GFP (green) in the pontine reticular nucleus, oral part (PnO) and supraleminiscal nucleus (SuL, B1), caudal linear nucleus (CLi, C1), raphe obscuris (ROb, D1), median raphe (MnR) and paramedian raphe (PMnR, E1), dorsal raphe nucleus (DRN, F1) and raphe magnus (RMg), raphe pallidus (RPa) and lateral paragiganticellular nucleus (LPGi, G1). Right: Pie charts depicting for each counted region the penetrance of Cre expression in 5HT i.r. neurons (i.e. the percent of 5HT i.r. neurons that expressed Cre-driven L10-GFP, purple shaded slice) and the specificity of Cre expression within each serotoninergic population (i.e. the percent of SERT-L10-GFP expressing neurons that were also 5HT i.r., green shaded slice). Scale bar: 100 μm. Abbreviations: Aq; aqueduct, ml; medial leminiscus, mlf; medial longitudinal fasciculus, py; pyramidal tract, xscp; decussation of the superior cerebellar peduncle.
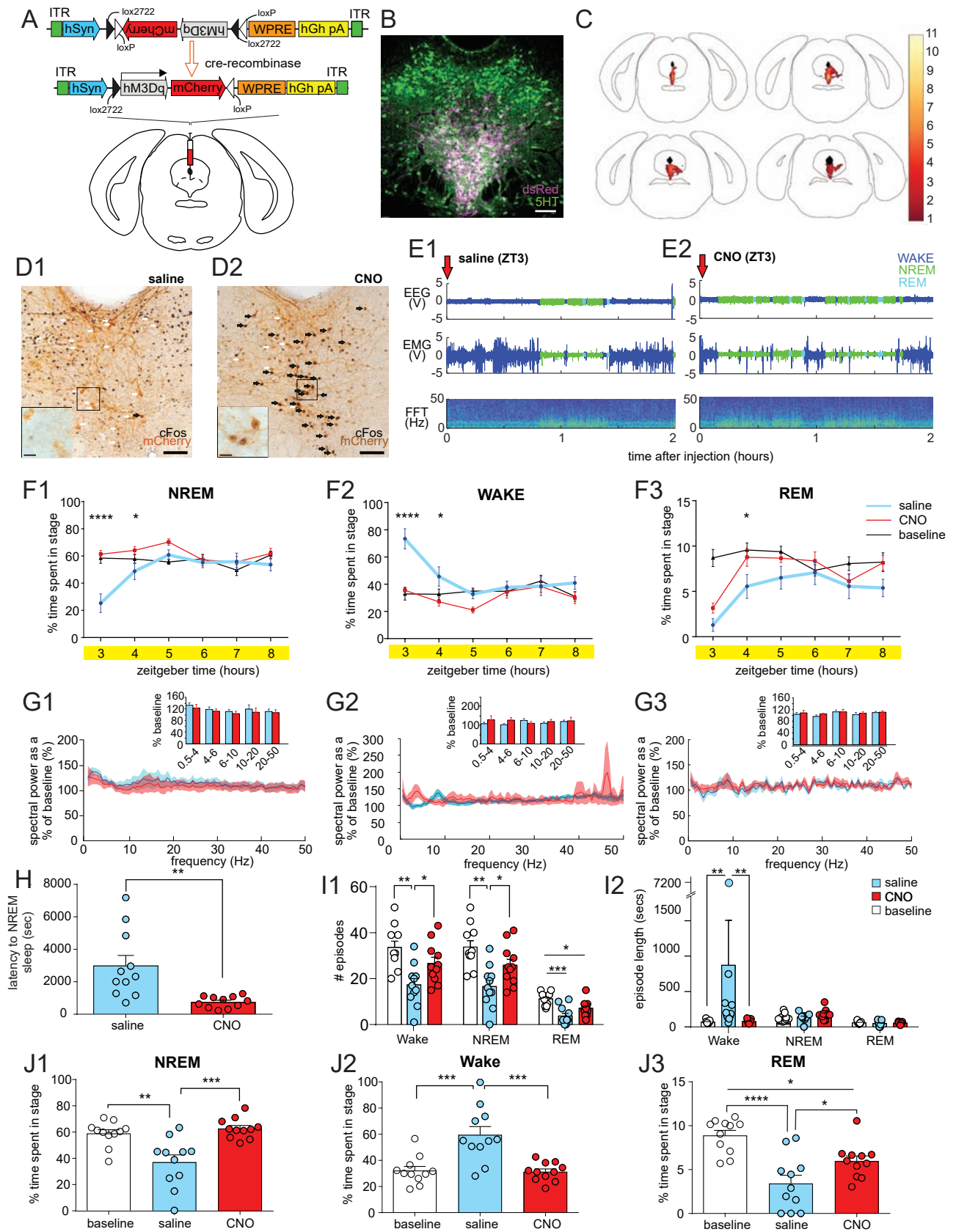
Figure 2. Conditional activation of DRN^SHT neurons reduces the latency to NREM sleep. (A) Schema of hSyn-FLEX-hM3Dq-mCherry-AAV10 construct and viral targeting to the DRN of SERT-cre mice. (B) Dual immunolabeling (white) against hM3Dq-mCherry (magenta) and 5HT (green) in DRN SERT+ cell bodies. Scale bar: 100 μm. (C) Heatmap illustrating overlapping regions of hM3Dq-Cherry-transduced neurons in SERT-Cre mice (*n* = 11). (D) Dual immunolabeling against hM3Dq-mCherry (brown)

L10-GFP expression was also observed in the thalamus and cingulate cortex as described previously, which likely reflects developmental expression of SERT [35].

We next placed injections of an AAV encoding the excitatory chemogenetic receptor, hSyn-FLEX-hM3Dq-mCherry-AAV10 (M3), into the DRN of SERT-Cre mice (Figure 2, A and B) to permit the reversible activation of DRN5HT (DRN5HT-M3) neurons while simultaneously performing polysomnography recordings. Transduced neurons were found in 31.8% ± 4.5% DRN5HT neurons ($n = 11$ mice) and were observed throughout the rostrocaudal extent of the DRN, but did not extend beyond its anatomical boundaries (Figure 2C). Injection of the hM3Dq ligand, CNO, elicited strong c-Fos expression (a marker of neuronal activity) in DRN5HT-M3 neurons, as compared with a control (saline) injection, demonstrating that DRN5HT-M3 neurons were specifically activated by CNO (Figure 2D; 86.7% ± 3.5% of hM3Dq neurons expressed c-Fos following CNO injection ($n = 4$ mice), compared with 1.2% ± 0.4% of hM3Dq neurons following a saline injection ($n = 4$ mice), $p < 0.0001$, independent sample t-test). Chemogenetic activation of DRN5HT-M3 neurons at ZT3 (9:00 am), a time approximating peak sleep drive in the mouse, significantly increased both NREM and REM sleep during the first 2 hours post-injection at the expense of wakefulness, but did not affect cortical spectral activity during any arousal state (Figure 2E–G). DRN5HT-M3 activation reduced the latency to the first episode of NREM following CNO injection (Figure 2H) and increased the number of transitions between wake and NREM sleep during the first 2 hours post-injection (Figure 2I). Of note, the amount of NREM sleep observed following CNO activation of DRN5HT neurons was comparable with NREM sleep levels observed in the same mice during baseline conditions, i.e. at the same time of day, but in the absence of an i.p. injection (Figure 2J), whereas REM sleep was slightly decreased. This finding suggests that the i.p. injection itself increases arousal, likely secondary to the effect of stress or anxiety caused produced by handling the mice [36]. It is plausible therefore that DRN5HT-M3 activation blunts this stress response, thereby facilitating the expression of normal sleep amounts at this time of day. Of note, no difference in sleep-wake parameters following CNO injection were observed in injection control mice that did not express the chemogenetic receptor (Supplementary Figure S1A–C), which is consistent with our previously reported data [37].

Activation of DRN5HT at ZT12 (6pm), a time of high waking drive in the mouse also increased NREM sleep, decreased the latency to the first episode of NREM sleep and shortened the length of wake episodes (albeit to a lesser degree), without affecting cortical spectral activity during any arousal state (Supplementary Figure S2A–F).

Acute activation of DRN5HT neurons is anxiolytic but does not increase locomotion or impact thermoregulation

To further investigate the hypothesis that DRN5HT neurons promote anxiolysis, we subjected the mice to both open field and elevated plus maze behavioral tests, while chemogenetically activating DRN5HT neurons (Figure 3A). All mice were awake throughout the duration of both the open field test and the elevated plus maze test. Following CNO administration, mice spent significantly more time in the center of the open field as compared to the saline condition (Figure 3B). This anxiolytic effect was not accompanied by significant changes in spontaneous locomotion, including distance traveled and velocity (Figure 3C). In contrast, CNO activation of DRN5HT neurons did not significantly change the amount of time spent in the open arm vs. the closed arm of the elevated plus maze or the number of open arm entries, and nor was any effect on distance traveled or velocity observed (Figure 3D). Administration of CNO in SERT-cre mice not bearing the hM3Dq receptor was without effect upon measures of anxiety (Supplementary Figure S1D and E).

Inhibition or ablation of central 5HT has been previously shown to disrupt temperature control [38, 39], whereas knockout of TpH2 in the midbrain and pons produces hyperactivity in a home cage environment [40]. To characterize acute effects of DRN5HT neurons upon body temperature (Tb) and locomotor activity (LMA), we chemogenetically activated these neurons while measuring Tb and LMA using implantable telemetric transmitters. Activation of DRN5HT neurons had no significant effect upon Tb or LMA at either ZT3 or ZT12 (Figure 3, E and F). The peak in Tb immediately following both the saline and CNO injection is typical of "handling artifact" and likely reflects mild stress-induced hyperthermia [41]. DRN5HT activation did not significantly reduce this stress-induced thermogenesis, suggesting that the anxiolytic effects of DRN5HT neurons do not extend to all physiological expressions of stress or anxiety. Of note, there was a slight reduction of LMA in CNO injected mice in the first hour following the ZT3 injection, likely reflecting the increased amount of time mice spent asleep following DRN5HT activation. However, this did not attain statistical significance in comparison with saline-injected mice, most likely because stationary wakefulness (e.g. grooming, a behavior commonly observed following handling) is not captured via telemetric LMA.

Discussion

Despite extensive study of the central serotoninergic system, a consensus view of its role in arousal control has remained lacking. Here we sought to determine the effect of acutely and

---

and c-Fos (black) in SERT-cre cell bodies after injection of saline (D1) or clozapine-N-oxide (CNO; D2) at ZT3, 90 minutes prior to sacrifice. Colocalization of mCherry and c-Fos (black filled arrows) was present in CNO injected mice, whereas c-Fos was not observed in hM3Dq-mCherry+ cells in saline-injected mice (black outlined arrows). Scale bars, 100 μm. Insets shows a higher magnification of the boxed area, scale bar: 20 μm. (E) Raw data examples showing EEG/EMG and spectrogram for 2 hours following the saline (E1) or CNO injection (E2). (F) Percentage of NREM sleep (F1), wake (F2), and REM sleep (F3) after ZT3 saline and CNO injection, and in the baseline condition ($n = 11$). Mean ± SEM, *$p < 0.05$, **$p < 0.01$, ****$p < 0.0001$, repeated-measures two-way ANOVA followed by Tukey's post hoc test. (G) Fast Fourier transform (FFT) analysis of NREM sleep (G1), wake (G2) and REM sleep (G3) following ZT3 saline and CNO injection ($n = 7$). Data is expressed as mean ratio of power at each frequency after injection compared with the baseline, shaded areas indicate SEM. Inserts show averaged frequency bands + SEM. Repeated-measures two-way ANOVA. (H) Latency to first episode of NREM sleep following injection of saline or CNO ($n = 11$). Mean + SEM, **$p < 0.01$, paired t-test. (I1) Number of wake, NREM sleep, and REM sleep episodes during the first 2 hours following ZT3 injection of saline or CNO and in the baseline condition ($n = 11$). Mean + SEM, *$p < 0.05$, **$p < 0.01$, repeated-measures one-way ANOVA followed by Tukey's post hoc test. (I2) Length of wake, NREM sleep, and REM sleep episodes during the first 2 hours following ZT3 injection of saline or CNO and in the baseline condition ($n = 11$). Mean + SEM, **$p < 0.01$, Friedman test followed by Dunn's multiple comparison tests. (J) Percentage of NREM sleep (J1), wake (J2), and REM sleep (J3) between ZT3 and ZT5 at baseline and following ZT3 injection of saline or CNO ($n = 11$). Mean + SEM, *$p < 0.05$, **$p < 0.01$, ***$p < 0.001$, ****$p < 0.0001$, one-way ANOVA.
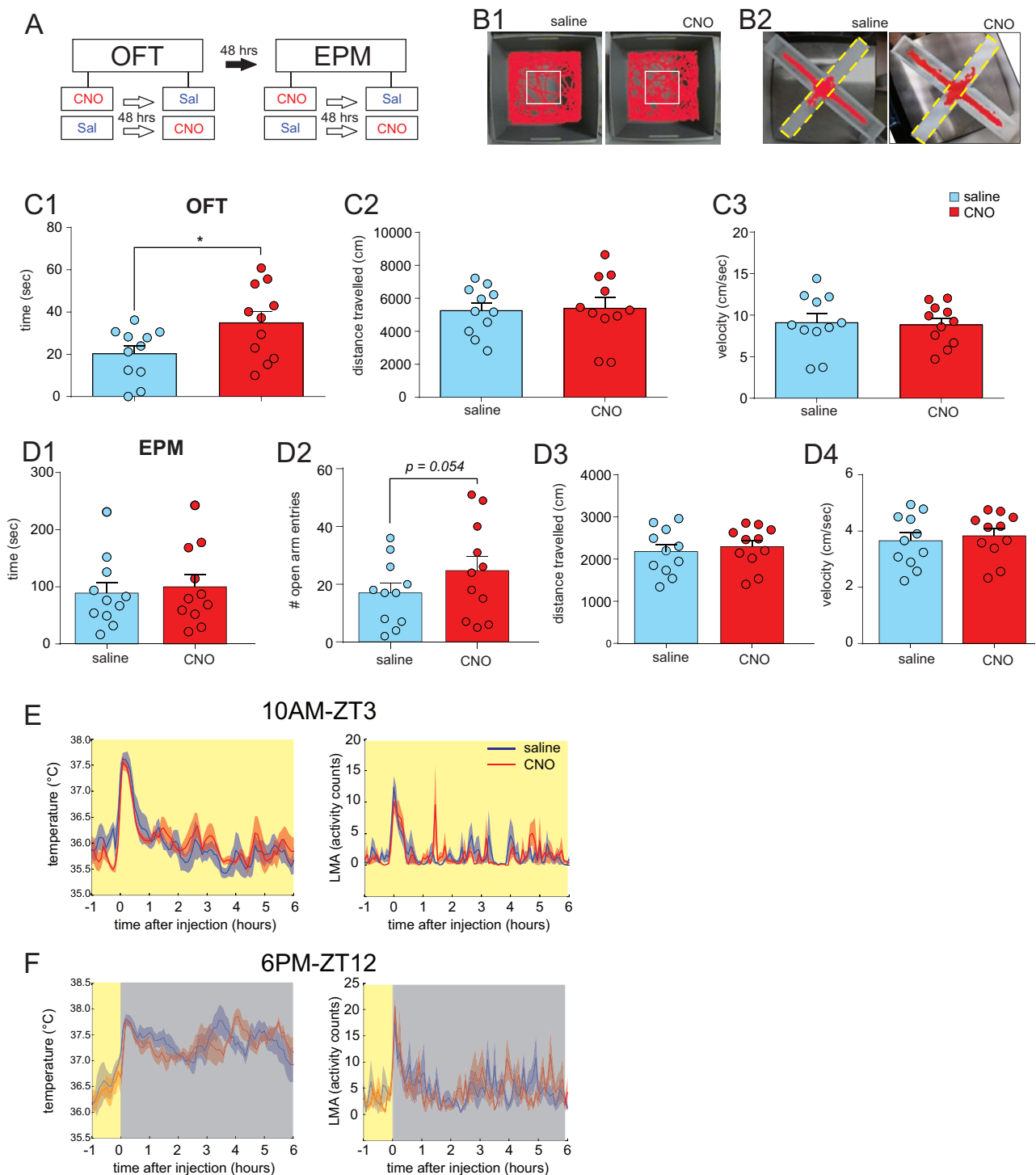
Figure 3. Acute activation of DRN^{5HT} neurons is anxiolytic but does not increase locomotion or impact thermoregulation. (A) Experimental plan of anxiety-related behavioral tests including the open field test (OFT) and the elevated plus maze (EPM). (B) Example Ethovision trace of mouse injected with saline vs. clozapine-N-oxide (CNO) in open field test (B1) and elevated plus maze (B2). The central area of the open field test is represented by the white box (B1) and the open arms of the elevated plus maze are show with yellow dashed lines (B2). (C) Time spent in the center of the open field test (C1), distance traveled (C2) and average velocity (C3), in mice injected with saline and CNO ($n = 11$). Mean + SEM, *$p < 0.05$, paired *t*-test. (D) Time spent in the open arm of the elevated plus maze test (D1), number of open arm entries (D2), distance traveled (D3), and average velocity (D4), following saline and CNO injection ($n = 11$). Mean + SEM, paired *t*-test. (E) Body temperature (left) and locomotor activity (LMA; right) following saline and CNO injection at ZT3 ($n = 5$). Mean ± SEM, repeated-measures two-way ANOVA. (F) Body temperature (left) and locomotor activity (LMA; right) following saline and CNO ($n = 5$) at ZT12. Mean ± SEM, repeated-measures two-way ANOVA.

selectively driving DRN^{5HT} neurons (utilizing a chemogenetic approach) upon sleep and wakefulness. Our major finding was that DRN^{5HT} activation briefly, but also significantly, increased NREM and REM sleep following injection of the chemogenetic ligand. However, the duration of NREM sleep following CNO-driven activation of DRN^{5HT} neurons was comparable to the duration of

NREM sleep during the same time period under baseline conditions (i.e. when mice are not injected with saline or CNO). Since a moderate increase in arousal is a well-known artifact of administering i.p. injections, likely associated with the mild stress that handling incurs upon the animal [42], this suggested to us the interesting possibility that DRN[5HT] activation dampens this stress-induced arousal and permits NREM sleep to occur to the same levels that are observed in the absence of a stressor. Consistent with this hypothesis, we showed that acute activation of DRN[5HT] neurons reduced anxiety behavior in the open field test. Altogether, our results suggest that acute activation of DRN[5HT] neurons does not drive NREM or REM sleep directly, but instead produces an anxiolytic effect that is sleep permissive in the setting of a stressor.

Curiously, we also found that DRN[5HT] activation increased REM sleep relative to the control i.p. saline condition but that the amount of REM sleep did not attain the levels observed at baseline (in the absence of an i.p. injection). As such, we cannot rule out the possibility that serotonergic activation may also be mildly REM-suppressing, as has been suggested previously [17, 18, 43, 44], although it is also plausible that mild stress is itself REM-suppressing.

With respect to prior reports in the literature, our results are inconsistent with the proposed wake-promoting role of DRN[5HT] neurons [16]. This hypothesis was largely informed by the high DRN neuron firing activity observed during the waking state [3–7], the extensive connectivity with other arousal centers [9–14] and the initial finding that 5HT is inhibitory at putative sleep-promoting neurons within the VLPO nucleus [15]. However, it is now established that 5HT has both excitatory and inhibitory actions at the VLPO nucleus [45, 46], and thus its role in suppressing sleep-promoting neurons is unclear. It is also the case that while DRN[5HT] neurons may exhibit a wake-active profile, such activity may not, in fact, be related to wake promotion, but rather to behaviors that occur during wakefulness. It is also worth noting that DRN[5HT] neurons innervate many other regions of the brain that have no known role in the regulation of arousal [12] and as such, are capable of modulating many other behaviors in addition to arousal.

Our findings appear consonant with those reported by Lu and colleagues [47], who found no significant changes in sleep or wake amounts following extensive (ca. 80%) cell-type specific lesions of the DRN[5HT] cell population. Our findings are also largely consistent—at least to the extent that they can be directly compared - with the recent report by Iwaskai and colleagues who generated a Pet-cre/DTA mouse line and found that central deletion of 5HT cell bodies was without effect on total wake or NREM sleep amounts, although a significant decrease in REM sleep amounts and an attenuated waking response following exposure to a novel environment was reported [48]. Seemingly contradictory results have been shown in studies employing 5HT receptor knockout mice that found effects on sleep-wake. For example, $5HT_{1A}$ and $5HT_{1B}$ receptor knock-out mice display increased REM sleep, suggesting that 5HT may suppress REM sleep via these receptors [17, 18], whereas selective knock-out of the $5HT_{1A}$ receptors in wake-stabilizing orexin neurons produces increased sleep [19]. However, it is possible that the apparent discrepancies between our findings and those in the knock-out studies may reflect ontogenetic or otherwise compensatory issues in the knockout mice. Another plausible explanation for the discrepancy between our findings and other published studies, in which interrogation was not limited to the DRN, is that the MnR nucleus may play a role in sleep-wake modulation. Similar to the DRN[5HT] population, serotoninergic MnR neurons also project widely to arousal centers [12, 14] whereas most 5HT neurons in the MnR nucleus exhibit a firing pattern that is negatively correlated with hippocampal theta rhythm [49, 50], although some MnR 5HT neurons have been identified that are phase-locked to hippocampal theta rhythm [51]. The role of MnR 5HT neurons in sleep-wake control is an important question for future investigation.

Dysfunction of the central 5HT system is a feature common to both sleep and mood disorders. To this end, SSRIs are a frequently employed and highly effective treatment for anxiety and depression in humans, but they also influence sleep, specifically REM sleep [52]. Consistent with the reported clinical efficacy of SSRIs for treating anxiety and depression, acute optogenetic activation of DRN[5HT] neurons generally biases mice towards reward-associated behaviors [53, 54]. Here, we show that chemogenetic activation of DRN[5HT] neurons produces a mild but significant reduction in anxiety per the open field test. This finding is interesting in light of other studies that have reported that acute chemogenetic activation of the entire brain 5HT system produces increased anxiogenic behavior [55], whereas chronic silencing of the global 5HT system reduces anxiogenic behavior [56]. An additional study reported that acute chemogenetic activation of DRN[5HT] neurons produced anxiogenic behavior, while chronic activation had no effect upon anxiety-like behavior but instead induced an anti-depressant responses during a forced swim test [57]. On the other hand, optogenetic activation of DRN[5HT] neurons suppressed locomotion in the open field test, without any effect upon measures of anxiety [58]. Given these disparate reports, 5HT's role in influencing behavioral states and vice versa has yet to be elucidated. However, a recent report has suggested the existence of two intermingled DRN[5HT] sub-systems, which differentially innervate the orbital frontal cortex (OFC) and the central amygdala (CeA). Gain and loss-of-function experiments in these two DRN[5HT] subpopulations revealed that more dorsally located CeA-projecting DRN[5HT] neurons increase anxiety whereas more ventrally located OFC-projecting DRN[5HT] neurons bear anxiolytic properties [59]. In our experiments, expression of the hM3Dq receptor extended both dorsally and ventrally throughout the DRN, and as such, it is likely that we activated both OFC- and CeA- projecting DRN[5HT] subpopulations. However, since we observed more consistent expression of hM3Dq in the more ventral regions of the DRN (Figure 2C), and activation of DRN[5HT] neurons in our hands was predominantly anxiolytic, we posit that we preferentially activated OFC-projecting DRN[5HT] neurons. Ultimately, our findings demonstrate that activation of DRN[5HT] neurons can decrease anxiety and thus favor NREM sleep under conditions of a mild stressor, such as administration of an i.p. injection. However, the neural circuitry through which DRN[5HT] neurons elicit these effects remains a question for future study.

Of note, although both the open field test and elevated plus maze are often used to study anxiety-related behavior in rodents [60], we report here that DRN[5HT] activation produced a significant anxiolytic effect in the open field test without a significant effect in the elevated plus maze. Several reasons could be attributed to this unexpected divergent finding. First, the open field test and elevated plus maze reflect different facets of emotionality [61]. Second, it is also important to consider the uncontrolled

individual fluctuations in behavior and/or emotional state at a certain point in time, which is inherent in using a series or battery of anxiety-related tests [62]. Furthermore, during an assessment of behavioral parameters in the open field test and elevated plus maze in different inbred mouse strains, C57BL/6 mice found the elevated plus maze more anxiogenic than the open field test [63]. Since our mice were bred on a C57BL/6 background [25], it is plausible that they may have found the EPM a more anxiogenic stimuli than the OFT and hence our presumptive anxiolysis (secondary to hM3Dq activation of DRN[5HT]) may not have been sufficient to produce a demonstrable decrease in anxiety on the EPM.

Technical considerations

Two technical points should be considered when interpreting our data. First, to manipulate DRN[5HT] neurons in a cell-type-specific manner, we required a Cre recombinase driver mouse line to gain genetic access to 5HT neurons. Of two SERT-Cre mouse lines [25, 64] and an ePet-Cre mouse line [65] available to us, we uncovered important limitations with two of these lines in our preliminary validation work. The SERT-Cre mouse line described by Zhang and colleagues utilized a knock-in approach to insert Cre just upstream of the first coding ATG of the SERT gene [64]. Unfortunately, this strategy renders the SERT allele null on the Cre-expressing allele. Since physiology is appreciably altered in SERT knock-out mice (even in the heterozygous condition [66]), and since SERT knock-out mice show increased amounts of REM sleep [67], we opted not to use this mouse line for carrying out our experimental work. The ePet-Cre mouse, in contrast, was developed by Scott and coworkers [65] and transcription and translation of the SERT gene is left undisturbed. However, in preliminary experiments we were unable to attain sufficient expression of Cre-dependent proteins following viral vector injections into the DRN (data not shown), hence we did not further pursue experimental work using the ePet-Cre mouse line. The third line of mice that we characterized and validated was the SERT-Cre mouse line that was generated as part of the GENSAT project [25]. This line exhibited excellent eutopic expression of Cre and strong expression of our Cre-dependent vectors.

A second consideration is our use of chemogenetics as a tool to activate DRN[5HT] neurons. Although chemogenetics offers many benefits, we must acknowledge some technical caveats. For example, DRN[5HT] neurons colocalize several neurotransmitters and small molecules [68], most notably, the glutamate transporter VGlut3, which would enable DRN[5HT] neurons to release glutamate upon activation [69, 70], and this glutamatergic transmission may have contributed to the effects upon sleep and anxiety that we observed. Additionally, the act of administering the chemogenetic ligand via i.p. injection is well-known to cause minor increases in arousal. Although we made a concerted effort to minimize this stress (by giving mock injections as per our protocol), it was impossible to completely eliminate. As such, one reasonable interpretation of our data was that activation of DRN[5HT] neurons enables sleep in the face of a mild stressor. It may also be conjectured that chemogenetic activation has the capacity to yield artificial and supra-physiological phenotypes. However, the rather modest increase in sleep we observed upon chemogenetic activation of DRN[5HT] neurons was well within the physiological range, arguing against this point of view.

Relatedly, we were unable to achieve expression of hM3Dq in all DRN[5HT] neurons. Although we observed consistent and robust responses to CNO administration in our mice, it is possible that a higher level of AAV-hM3Dq transfection (and hence hM3Dq expression) would have produced even greater magnitude responses in our measured variables, e.g. a significant EPM test result. Alternatively, increasing the extent of the transduced neurons (particularly in the more dorsal, CeA-projecting regions of the DRN [59]) could have yielded an opposite sleep-wake phenotype. We nevertheless consider our approach to be one of many strengths, in particular, the ability to achieve acute and selective activation of DRN[5HT] neurons in behaving mice, and the general absence of ontogenetic considerations that are inherent to other development transgenic models.

Concluding remarks

To the best of our knowledge we have, for the first time, interrogated DRN[5HT] neurons selectively, and in an acute manner, with a specific and unbiased emphasis on behavioral state regulation. When considered in the framework of the existing literature, our experimental findings argue the more nuanced perspective that DRN[5HT] may not modulate sleep-wake per se, but rather that their activation is sleep permissive under circumstances that produce anxiety or stress.

Supplementary Material

Supplementary material is available at *SLEEP* online.

Figure S1. Administration of the chemogenetic ligand in mice that do not express the hM3Dq receptor does not impact sleep-wake parameters or measures of anxiety. A. Percentage of NREM sleep (A1), wake (A2), and REM sleep (A3) after ZT3 saline and clozapine-N-oxide (CNO) injection (n = 7). Mean + SEM, repeated-measures two-way ANOVA. B. Latency to first episode of NREM sleep following injection of saline or CNO (n = 7). Mean + SEM, paired t-test. C. Number (C1) and length (C2) of wake, NREM sleep and REM sleep episodes during the first two hours following ZT3 injection of saline or CNO (n =7). Mean + SEM, paired t-test. D. Time spent in the center of the open field test (D1), distance traveled (D2) and average velocity (D3), in mice injected with saline and CNO (n=9). Mean + SEM, paired t-test. E. Time spent in the open arm of the elevated plus maze test (E1), number of open arm entries (E2) distance traveled (E3), and average velocity (E4), following saline and CNO injection (n=9). Mean + SEM, paired t-test.

Figure S2. Activation of DRN[5HT] neurons in the evening moderately increases NREM sleep. A. Raw data examples showing EEG/EMG and spectrogram for two hours following ZT12 saline (A1) or clozapine-N-oxide (CNO) injection (A2). B. Percentage of NREM sleep (F1), wake (F2), and REM sleep (F3) after ZT12 saline and CNO injection (n=10). Mean ± SEM, ** $p<0.01$, repeated-measures two-way ANOVA followed by Sidak post hoc test. C. Fast Fourier transform (FFT) analysis of NREM sleep (C1), wake (C2) and REM sleep (C3) following ZT12 saline and CNO injection (n=6). Data is expressed as mean ratio of power at each frequency after injection compared with the baseline, shaded areas indicate SEM. Inserts show averaged frequency bands + SEM. Repeated-measures two-way ANOVA. D. Latency to first episode of NREM sleep following injection of saline or CNO (n = 10). Mean + SEM, * $p<0.015$ paired t-test. E. Number (E1) and length (E2) of wake, NREM sleep and

REM sleep episodes during the first two hours following ZT12 injection of saline or CNO (n =10). Mean + SEM, * *p*<0.05, paired t-test. F. Percentage of NREM sleep (F1), wake (F2), and REM sleep (F3) between ZT12 and ZT14 at baseline and following ZT12 injection of saline or CNO (n=10). Mean + SEM, one-way ANOVA.

References

1. Müller C, *et al. Handbook of the Behavioral Neurobiology of Serotonin*. San Diego, CA: Elsevier; 2010.
2. Jouvet M. The role of monoamines and acetylcholine-containing neurons in the regulation of the sleep-waking cycle. *Ergeb Physiol*. 1972;**64**:166–307.
3. McGinty DJ, *et al*. Dorsal raphe neurons: depression of firing during sleep in cats. *Brain Res*. 1976;**101**(3):569–575.
4. Shima K, *et al*. Firing properties of two types of nucleus raphe dorsalis neurons during the sleep-waking cycle and their responses to sensory stimuli. *Brain Res*. 1986;**399**(2):317–326.
5. Trulson ME, *et al*. Raphe unit activity in freely moving cats: correlation with level of behavioral arousal. *Brain Res*. 1979;**163**(1):135–150.
6. Urbain N, *et al*. Electrophysiological diversity of the dorsal raphe cells across the sleep-wake cycle of the rat. *J Physiol*. 2006;**573**(Pt 3):679–695.
7. Sakai K, *et al*. Differentiation of presumed serotonergic dorsal raphe neurons in relation to behavior and wake-sleep states. *Neuroscience*. 2001;**104**(4):1141–1155.
8. Portas CM, *et al*. Serotonin and the sleep/wake cycle: special emphasis on microdialysis studies. *Prog Neurobiol*. 2000;**60**(1):13–35.
9. Ogawa SK, *et al*. Organization of monosynaptic inputs to the serotonin and dopamine neuromodulatory systems. *Cell Rep*. 2014;**8**:1105–1118.
10. Pollak Dorocic I, *et al*. A whole-brain atlas of inputs to serotonergic neurons of the dorsal and median raphe nuclei. *Neuron*. 2014;**83**(3):663–678.
11. Weissbourd B, *et al*. Presynaptic partners of dorsal raphe serotonergic and GABAergic neurons. *Neuron*. 2014;**83**(3):645–662.
12. Bang SJ, *et al*. Projections and interconnections of genetically defined serotonin neurons in mice. *Eur J Neurosci*. 2012;**35**(1):85–96.
13. Chou TC, *et al*. Afferents to the ventrolateral preoptic nucleus. *J Neurosci*. 2002;**22**(3):977–990.
14. Muzerelle A, *et al*. Conditional anterograde tracing reveals distinct targeting of individual serotonin cell groups (B5-B9) to the forebrain and brainstem. *Brain Struct Funct*. 2016;**221**(1):535–561.
15. Gallopin T, *et al*. Identification of sleep-promoting neurons in vitro. *Nature*. 2000;**404**(6781):992–995.
16. Saper CB, *et al*. Sleep state switching. *Neuron*. 2010;**68**(6):1023–1042.
17. Boutrel B, *et al*. Key role of 5-HT1B receptors in the regulation of paradoxical sleep as evidenced in 5-HT1B knock-out mice. *J Neurosci*. 1999;**19**(8):3204–3212.
18. Boutrel B, *et al*. Involvement of 5-HT1A receptors in homeostatic and stress-induced adaptive regulations of paradoxical sleep: studies in 5-HT1A knock-out mice. *J Neurosci*. 2002;**22**(11):4686–4692.
19. Saito YC, *et al*. Serotonergic input to orexin neurons plays a role in maintaining wakefulness and REM sleep architecture. *Front Neurosci*. 2018;**12**:892.
20. Monti JM. The role of dorsal raphe nucleus serotonergic and non-serotonergic neurons, and of their receptors, in regulating waking and rapid eye movement (REM) sleep. *Sleep Med Rev*. 2010;**14**(5):319–327.
21. Johnson EO, *et al*. The association of insomnia with anxiety disorders and depression: exploration of the direction of risk. *J Psychiatr Res*. 2006;**40**(8):700–708.
22. Mendlewicz J. Sleep disturbances: core symptoms of major depressive disorder rather than associated or comorbid disorders. *World J Biol Psychiatry*. 2009;**10**(4):269–275.
23. Shaffery J, *et al*. The neurobiology of depression: perspectives from animal and human sleep studies. *Neuroscientist*. 2003;**9**(1):82–98.
24. Hertenstein E, *et al*. Insomnia as a predictor of mental disorders: a systematic review and meta-analysis. *Sleep Med Rev*. 2019;**43**:96–105.
25. Gong S, *et al*. Targeting Cre recombinase to specific neuron populations with bacterial artificial chromosome constructs. *J Neurosci*. 2007;**27**(37):9817–9823.
26. Krashes MJ, *et al*. An excitatory paraventricular nucleus to AgRP neuron circuit that drives hunger. *Nature*. 2014;**507**(7491):238–242.
27. Schindelin J, *et al*. Fiji: an open-source platform for biological-image analysis. *Nat Methods*. 2012;**9**(7):676–682.
28. Hornung JP. The neuroatomy of the serotonergic system. In: Müller C, Jacobs B, eds. *Handbook of the Behavioral Neurobiology of Serotonin*. San Diego, CA: Elsevier; 2010: 51–64.
29. Dahlstroem A, *et al*. Evidence for the existence of monoamine-containing neurons in the central nervous system. I. Demonstration of monoamines the cell bodies of brain stem neurons. *Acta Physiol. Scand*. 1964;**232**:1–55.
30. Vertes RP, *et al*. Distribution, quantification, and morphological characteristics of serotonin-immunoreactive cells of the supralemniscal nucleus (B9) and pontomesencephalic reticular formation in the rat. *J Comp Neurol*. 1997;**378**(3): 411–424.
31. Franklin KBJ, *et al. The Mouse Brain in Stereotaxic Coordinates*. 3rd edition. New York, NY: Elsevier; 2008.
32. Amaral DG, *et al*. An air pressure system for the injection of tracer substances into the brain. *J Neurosci Methods*. 1983;**9**(1):35–43.
33. Anaclet C, *et al*. Basal forebrain control of wakefulness and cortical rhythms. *Nat Commun*. 2015;**6**:8744.
34. Venner A, *et al*. A novel population of wake-promoting GABAergic neurons in the ventral lateral hypothalamus. *Curr Biol*. 2016;**26**(16):2137–2143.
35. Lebrand C, *et al*. Transient developmental expression of monoamine transporters in the rodent forebrain. *J Comp Neurol*. 1998;**401**(4):506–524.

36. Ryabinin AE, *et al*. Different levels of Fos immunoreactivity after repeated handling and injection stress in two inbred strains of mice. *Pharmacol Biochem Behav*. 1999;**63**(1):143–151.

37. Anaclet C, *et al*. The GABAergic parafacial zone is a medullary slow wave sleep-promoting center. *Nat Neurosci*. 2014;**17**(9):1217–1224.

38. Ray RS, *et al*. Impaired respiratory and body temperature control upon acute serotonergic neuron inhibition. *Science*. 2011;**333**(6042):637–642.

39. Murray NM, *et al*. Insomnia caused by serotonin depletion is due to hypothermia. *Sleep*. 2015;**38**(12):1985–1993.

40. Whitney MS, *et al*. Adult brain serotonin deficiency causes hyperactivity, circadian disruption, and elimination of siestas. *J Neurosci*. 2016;**36**(38):9828–9842.

41. Meijer MK, *et al*. Effect of restraint and injection methods on heart rate and body temperature in mice. *Lab Anim*. 2006;**40**(4):382–391.

42. Lapin IP. Only controls: effect of handling, sham injection, and intraperitoneal injection of saline on behavior of mice in an elevated plus-maze. *J Pharmacol Toxicol Methods*. 1995;**34**(2):73–77.

43. Berger M, *et al*. Symposium: normal and abnormal REM sleep regulation: REM sleep in depression-an overview. *J Sleep Res*. 1993;**2**(4):211–223.

44. McCarley RW. Neurobiology of REM and NREM sleep. *Sleep Med*. 2007;**8**:302–330.

45. Gallopin T, *et al*. Effect of the wake-promoting agent modafinil on sleep-promoting neurons from the ventrolateral preoptic nucleus: an in vitro pharmacologic study. *Sleep*. 2004;**27**(1):19–25.

46. Sangare A, *et al*. Serotonin differentially modulates excitatory and inhibitory synaptic inputs to putative sleep-promoting neurons of the ventrolateral preoptic nucleus. *Neuropharmacology*. 2016;**109**:29–40.

47. Lu J, *et al*. A putative flip-flop switch for control of REM sleep. *Nature*. 2006;**441**(7093):589–594.

48. Iwasaki K, *et al*. Ablation of central serotonergic neurons decreased REM sleep and attenuated arousal response. *Front Neurosci*. 2018;**12**:535.

49. Domonkos A, *et al*. Divergent in vivo activity of non-serotonergic and serotonergic VGluT3-neurones in the median raphe region. *J Physiol*. 2016;**594**(13):3775–3790.

50. Viana Di Prisco G, *et al*. Discharge properties of neurons of the median raphe nucleus during hippocampal theta rhythm in the rat. *Exp. Brain Res*. 2002;**145**:383–394. doi:10.1007/s00221-002-1123-8

51. Kocsis B, *et al*. Serotonergic neuron diversity: identification of raphe neurons with discharges time-locked to the hippocampal theta rhythm. *Proc Natl Acad Sci U S A*. 2006;**103**(4):1059–1064.

52. Palagini L, *et al*. REM sleep dysregulation in depression: state of the art. *Sleep Med Rev*. 2013;**17**(5):377–390.

53. Liu Z, *et al*. Dorsal raphe neurons signal reward through 5-HT and glutamate. *Neuron*. 2014;**81**(6):1360–1374.

54. Li Y, *et al*. Serotonin neurons in the dorsal raphe nucleus encode reward signals. *Nat Commun*. 2016;**7**:10503.

55. Teissier A, *et al*. Activity of raphé serotonergic neurons controls emotional behaviors. *Cell Rep*. 2015;**13**(9):1965–1976.

56. Kim JC, *et al*. Linking genetically defined neurons to behavior through a broadly applicable silencing allele. *Neuron*. 2009;**63**(3):305–315.

57. Urban DJ, *et al*. Elucidation of the behavioral program and neuronal network encoded by dorsal raphe serotonergic neurons. *Neuropsychopharmacology*. 2016;**41**(5):1404–1415.

58. Correia PA, *et al*. Transient inhibition and long-term facilitation of locomotion by phasic optogenetic activation of serotonin neurons. *eLife*. 2017;**6**:e20975. doi:10.7554/eLife.20975

59. Ren J, *et al*. Anatomically defined and functionally distinct dorsal raphe serotonin sub-systems. *Cell*. 2018;**175**(2):472–487.e20.

60. Donner NC, *et al*. Sex differences in anxiety and emotional behavior. *Pflugers Arch*. 2013;**465**(5):601–626.

61. Rodgers RJ. Animal models of 'anxiety': where next? *Behav Pharmacol*. 1997;**8**(6-7):477–96; discussion 497.

62. Ramos A. Animal models of anxiety: do I need multiple tests? *Trends Pharmacol Sci*. 2008;**29**(10):493–498.

63. Carola V, *et al*. Evaluation of the elevated plus-maze and open-field tests for the assessment of anxiety-related behaviour in inbred mice. *Behav Brain Res*. 2002;**134**(1-2):49–57.

64. Zhuang X, *et al*. Targeted gene expression in dopamine and serotonin neurons of the mouse brain. *J Neurosci Methods*. 2005;**143**(1):27–32.

65. Scott MM, *et al*. A genetic approach to access serotonin neurons for in vivo and in vitro studies. *Proc Natl Acad Sci U S A*. 2005;**102**(45):16472–16477.

66. Murphy DL, *et al*. Targeting the murine serotonin transporter: insights into human neurobiology. *Nat Rev Neurosci*. 2008;**9**(2):85–96.

67. Wisor JP, *et al*. Altered rapid eye movement sleep timing in serotonin transporter knockout mice. *Neuroreport*. 2003;**14**(2):233–238.

68. Fu W, *et al*. Chemical neuroanatomy of the dorsal raphe nucleus and adjacent structures of the mouse brain. *J Comp Neurol*. 2010;**518**(17):3464–3494.

69. Gras C, *et al*. A third vesicular glutamate transporter expressed by cholinergic and serotoninergic neurons. *J Neurosci*. 2002;**22**(13):5442–5451.

70. Qi J, *et al*. A glutamatergic reward input from the dorsal raphe to ventral tegmental area dopamine neurons. *Nat Commun*. 2014;**5**:5390.